GMR
The Original

NETWORK PHARMACOLOGY AND MOLECULAR DYNAMIC EVALUATION OF MYCELIA -DERIVED QUINOLINE AGAINST NON-ALCOHOLIC FATTY LIVER DISEASE

Apeksha Rathi[1], Ekta Bhatt[2], Chakresh Kumar Jain[3]

[1,2,3]Department of Biotechnology, Jaypee Institute of Information Technology, A-10 Sector-62, Noida, India
*Corresponding author's email: chakresh.jain@mail.jiit.ac.in

ABSTRACT

Non-Alcoholic Fatty Liver Disease (NAFLD) is a progressive metabolic disorder associated with hepatic lipid accumulation, oxidative stress, inflammation, and fibrosis. Due to the limited availability of effective pharmacological therapies, exploration of novel bioactive compounds with multi-target therapeutic potential has become increasingly important[1]. In the present study, an integrated computational approach involving Gas Chromatography–Mass Spectrometry (GC–MS), network pharmacology, molecular docking, and molecular dynamics (MD) simulation was employed to investigate the therapeutic potential of quinoline-associated heterocyclic compounds identified from the mycelial extracts of *Ganoderma lucidum* and *Hericium erinaceus* against NAFLD.

GC–MS analysis revealed the presence of quinoline and its derivatives, indicating the occurrence of alkaloid-like bioactive metabolites. Network pharmacology analysis identified 69 overlapping targets associated with inflammatory and metabolic pathways involved in NAFLD progression. Gene Ontology and KEGG pathway enrichment analyses demonstrated significant involvement of TNF signaling, oxidative stress response, and lipid metabolism pathways. Molecular docking analysis showed favorable interaction between quinoline and TNF-α protein (PDB ID: 2AZ5), with a binding affinity score of −5.9 kcal/mol. Furthermore, MD simulation confirmed the structural stability of the quinoline–TNF-α complex through stable RMSD, RMSF, Rg, SASA, PCA, and FEL profiles. Overall, the findings suggest that quinoline-associated heterocyclic compounds may serve as promising therapeutic candidates against NAFLD.

KEYWORDS: Quinoline, NAFLD, Network Pharmacology, Molecular Docking, Molecular Dynamics Simulation

1. INTRODUCTION

Non-Alcoholic Fatty Liver Disease (NAFLD) has become a leading cause of chronic liver disorders worldwide, driven largely by the rising prevalence of obesity, insulin resistance, and metabolic syndrome[1]. It encompasses a progressive spectrum ranging from simple hepatic steatosis to non-alcoholic steatohepatitis (NASH), which may advance to fibrosis, cirrhosis, and hepatocellular carcinoma[2]. Although NAFLD develops in the absence of significant alcohol intake, it shares several pathological mechanisms with Alcoholic Liver Disease (ALD), including lipid accumulation, oxidative stress, mitochondrial dysfunction, and persistent inflammation[3]. These inter-connected processes contribute to hepatocellular injury and disease progression[4].

The pathogenesis of NAFLD is multifactorial and involves dysregulation of lipid metabolism, excessive free fatty acid influx, and impaired β-oxidation[5]. These alterations promote lipotoxicity and trigger the generation of reactive oxygen species (ROS), leading to oxidative damage and activation of inflammatory pathways[6]. Pro-inflammatory mediators such as tumor necrosis factor-α (TNF-α) and various interleukins further amplify hepatic inflammation[7], while chronic cellular stress stimulates fibrogenesis through activation of hepatic stellate cells[8]. Despite extensive research, effective pharmacological interventions targeting these complex mechanisms remain limited, necessitating the exploration of multi-target therapeutic strategies[9].

Medicinal mushrooms have long been recognized as valuable sources of bioactive metabolites possessing antioxidant, anti-inflammatory, hepatoprotective, and immunomodulatory properties[10]. Among these, *Ganoderma lucidum* and *Hericium erinaceus* are widely studied due to their rich phytochemical composition and therapeutic significance[11]. Several secondary metabolites isolated from mushroom mycelia have demonstrated potential in modulating metabolic and inflammatory disorders[12]. The identification of novel heterocyclic compounds from fungal sources may therefore contribute toward the development of alternative therapeutic agents against complex diseases such as NAFLD[13].

In recent years, nitrogen-containing heterocyclic compounds have attracted considerable attention because of their structural diversity and broad spectrum of biological activities. Quinoline, a nitrogen-containing heterocyclic aromatic compound (C_9H_7N), represents an important pharmacophore in medicinal chemistry[14]. Quinoline derivatives have been reported to exhibit anti-inflammatory, antioxidant, antimicrobial, anticancer, and metabolic regulatory activities[15]. The structural adaptability of quinoline enables its interaction with diverse biological targets involved in oxidative stress, inflammatory signalling, and metabolic imbalance[16].

In the present study, quinoline identified from the mycelial extracts of *Ganoderma lucidum* and *Hericium Erinaceus* through GC-MS analysis was investigated for its therapeutic potential against NAFLD using an integrated computational strategy[17]. Network pharmacology was employed to identify disease-associated targets and signalling pathways, followed by protein–protein interaction analysis and functional enrichment studies[18]. Molecular docking and molecular dynamics simulation were further performed to evaluate the binding affinity and structural stability of quinoline against TNF-α. The study provides mechanistic insights into the therapeutic relevance of mushroom-derived quinoline in NAFLD and establishes a computational basis for future experimental investigations[19].

2. MATERIALS AND METHODS

2.1 Identification of Quinoline by GC-MS Analysis

Mycelial extracts of *Ganoderma lucidum* and *Hericium erinaceus* were subjected to Gas Chromatography–Mass Spectrometry (GC-MS) analysis for the identification of bioactive metabolites[20]. The ethanolic extracts obtained from the mushroom mycelia were subjected to Gas Chromatography–Mass Spectrometry (GC–MS) analysis for the identification and characterization of bioactive constituents present in each sample. GC–MS analysis was performed using a Shimadzu QP-2010 Plus GC–MS system at the Advanced Instrumentation Research Facility (AIRF), Jawaharlal Nehru University (JNU), following the manufacturer's recommended tuning procedures to ensure optimal mass accuracy and instrument sensitivity. No internal standard was used during the analysis[20].

Chromatographic separation was achieved using an HP-5 MS capillary column (30 m × 0.25 mm i.d., 0.25 µm film thickness; 5% phenyl methyl siloxane). Helium served as the carrier gas at a constant flow rate of 1.61 mL/min with a split ratio of 1:10. The oven temperature program was initiated at 60°C and maintained for 2 min, followed by a temperature increase to 250°C at a rate of 20°C/min and held at the final temperature for 10 min. The ion source temperature was maintained at 250°C, while electron ionization (EI) was carried out at 70 eV. A sample volume of 1 µL of the ethanolic extract was injected into the GC–MS system for analysis.

Compound identification was performed by matching the obtained mass spectra with those available in Dr. Duke database[20, 21,22]. Spectral database and the GC–MS mass spectral library integrated with the Shimadzu QP-2010 Plus system at AIRF, JNU. The identified compounds were catalogued and summarized in tabular form. Relative quantification of the detected metabolites was achieved using the peak area normalization method, and the abundance of each compound was expressed as a percentage of the total ion chromatogram (TIC).Quinoline was identified as one of the significant nitrogen-containing heterocyclic compounds present in the mushroom mycelial extracts.

2.2 Retrieval of Chemical Structure and Target Prediction

The chemical structure of quinoline was retrieved from the PubChem database in SDF format for computational analysis (https://pubchem.ncbi.nlm.nih.gov/).Potential molecular targets associated with quinoline were predicted using the Traditional Chinese Medicine Systems Pharmacology (TCMSP) platform. The identified targets were standardized using UniProt database annotations[23].

2.3 Identification of NAFLD-Associated Genes

Genes associated with Non-Alcoholic Fatty Liver Disease (NAFLD) were identified using the Comparative Toxicogenomics Database (CTD) Comparative toxicogenomic (http://ctdbase.org/). Disease-related targets were screened and compiled for further comparative analysis. Common targets between quinoline-associated proteins and NAFLD-associated genes were identified using Venn-based intersection analysis[24].

2.4 Protein–Protein Interaction Network Construction

The overlapping targets were imported into the STRING database to construct a Protein–Protein Interaction (PPI) network. The interaction network was visualized and analyzed using Cytoscape software. Hub genes were identified based on network topology parameters, including degree centrality and interaction scores. A total 69 targets of quinoline were uploaded to the STRING database[25], with the species set to *Homo sapiens*. The protein–protein interaction network was generated, and results were imported into Cytoscape for better visualization and analysis. STRING links even non-interacting proteins, such as inhibitors and activators within the same pathway[25].

2.5 Gene Ontology and Pathway Enrichment Analysis

Functional enrichment analysis of the common targets was carried out using the WebGestalt platform. Gene Ontology (GO) enrichment analysis was performed to identify significant biological processes, molecular functions, and cellular components associated with the selected targets. Kyoto Encyclopedia of Genes and Genomes (KEGG) pathway enrichment analysis was also conducted to identify major signaling pathways involved in NAFLD pathogenesis[26].

2.6 Compound–Target–Pathway Network Construction

A compound–target–pathway interaction network was constructed to visualize the relationship between quinoline, disease-associated targets, and enriched signaling pathways. Cytoscape was used to visualize the compound–target–pathway network and explore the interactions between linoleic acid-associated targets and enriched biological pathways. This network analysis helped identify key molecular interactions potentially involved in disease regulation.The network was analyzed to identify key molecular interactions potentially involved in the therapeutic effects of quinoline against NAFLD[27].

2.7 Molecular Docking Analysis

Molecular docking analysis was performed to evaluate the binding affinity between quinoline and TNF-α protein. The three-dimensional crystal structure of TNF-α (PDB ID: 2AZ5) was retrieved from the Protein Data Bank (PDB). Protein preparation involved removal of water molecules, addition of hydrogen atoms, and energy minimization. Quinoline structure preparation and docking simulations were conducted using AutoDock Vina software. Binding affinity scores were calculated in kcal/mol, and docked conformations were analyzed using molecular visualization tools[28].

2.8 Molecular Dynamics Simulation

To investigate the stability of the protein–ligand complex, molecular dynamics (MD) simulation was performed for 200 ns. The docked TNF-α–quinoline complex was subjected to simulation under appropriate temperature and pressure conditions. Structural stability and conformational behavior of the complex were analyzed using parameters including Root Mean Square Deviation (RMSD), Root Mean Square Fluctuation (RMSF), Radius of Gyration (Rg), Solvent Accessible Surface Area (SASA), hydrogen bond analysis, Principal Component Analysis (PCA), and Free Energy Landscape (FEL) analysis[29]. We prepare the complex for MDS by applying the charmm-36 July 2022 forcefield, periodic boundary condition. Solvation and neutralization were done followed by energy minimization. It was found that the average potential energy of the system post energy minimization was -4.82342e+5kJ/mol which states the structure is stable post energy minimization. Equilibration was performed on the system and a constant temperature of '300 K' and constant pressure of '-0.631283bar' was obtained accepted (temperature range is 290K to 310K while pressure is -50 to +50 bar respectively). Both temperature and pressure equilibration were achieved at 1000ps. MDS was performed for 200ns and trajectory was studied to find RMSD, RMSF, Radius of Gyration of the system and MM-PBSA.

3. RESULTS AND DISCUSSION

3.1 Identification of Quinoline from Mushroom Mycelia

GC-MS analysis of the mycelial extracts of *Ganoderma lucidum* and *Hericium erinaceus* revealed the presence of several bioactive compounds, among which quinoline was identified as a significant nitrogen-containing heterocyclic compound. The presence of quinoline in medicinal mushroom mycelia suggests its possible contribution to the therapeutic properties traditionally associated with these fungi. For obtaining the chemical structure of Linoleic acid and formula PubChemdatabase was used Molecular Formula- C_9H_7N Molecular Weight- 129.16 g/mol

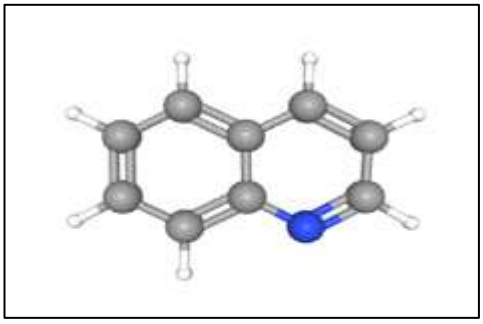

Figure 1- 3d structure of quinoline

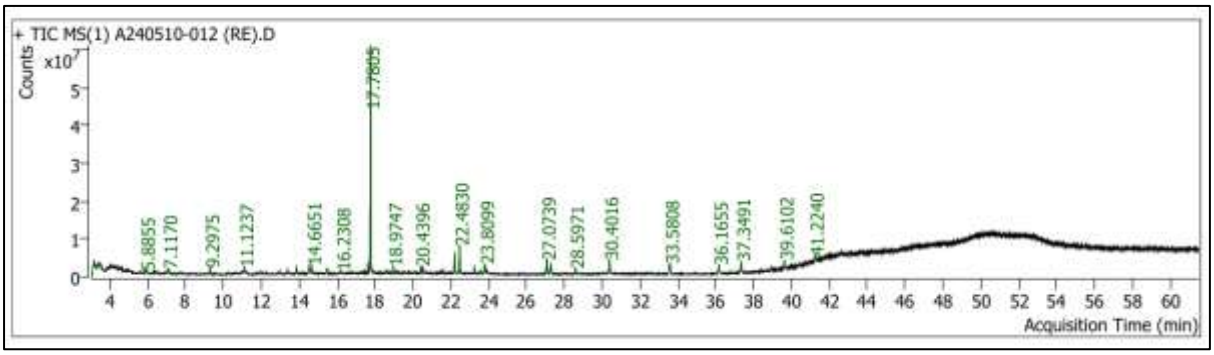

Figure-2 graphical representation of bioactive compounds identified by GC-MS in Ganoderma lucidium

Table-1 GC–MS chromatogram of Ganoderma lucidum mycelial extract showing the presence of key bioactive compounds.

Peak	Retention Time	Area	Area %	Compound Name	Molecular formula	Molecular weight	Compound activity	references
1.	3.1703	19848018.3	15.4	2-Phenylethyl isopropyl ether	C11H16O	164.24	Aromatic ether; reported antimicrobial and	[22]

							flavouring properties	
2.	3.4586	10347261.4	8.0	Toluene	C7H8	92.14	Industrial solvent; antimicrobial activity reported in some extracts	[22]
3.	5.8855	2612682.2	2.0	Benzene, 1-bromo-4-	C6H5Br	157.01	Halogenated aromatic compound; intermediate in pharmaceutical synthesis	[22]
4.	7.1170	6803141.7	5.3	Mesitylene	C9H12	120.19	Aromatic hydrocarbon with antioxidant and solvent applications	[22]
5.	9.2975	4094116.9	3.2	Linalool	C10H18O	154.25	Anti-inflammatory, antioxidant, antimicrobial activity	[22]
6.	10.3067	3743363.5	2.9	Cyclopentasiloxane, decamethyl-	C10H30O5Si5	370.77	Silicone-based compound; used in cosmetics and pharmaceutical formulations	[22]
7.	11.1237	7574629.0	5.9	2,4-Difluorobenzene, 1-	C6H4F2	114.09	Fluorinated aromatic compound; pharmaceutical intermediate	[22]
8.	12.0247	1797282.0	1.4	Benzaldehyde, 4-(1-methylethyl)-	C10H12O	148.20	Antimicrobial and fragrance-related applications	[22]
9.	13.8584	3998569.7	3.1	Benzene, 1,2,3-trichloro-4-methyl-	C7H5Cl3	195.47	Halogenated aromatic compound; industrial intermediate	[22]
10.	14.5377	4987347.1	3.9	Behenic alcohol	C22H46O	326.60	Emollient, antimicrobial and anti-inflammatory potential	[22]
11.	14.6651	7488407.7	5.8	Decane, 5-methyl-	C11H24	156.31	Hydrocarbon reported in bioactive plant and fungal extracts	[22]
12.	15.4718	1821650.4	1.4	Cyclohexane, octyl-	C14H28	196.37	Hydrophobic hydrocarbon with possible antimicrobial role	[22]

13.	15.5143	2787873.7	2.2	Quinoline, 1,2-dihydro-2,2,4-trimethyl-	C12H15N	173.25	Quinoline derivative with anti-inflammatory, antioxidant, and pharmacological potential	[22]
14.	16.2308	2498242.5	1.9	Cycloheptasiloxane,	C14H42O7Si7	518.99	Silicone compound used in pharmaceutical and cosmetic formulations	[22]
15.	17.6479	4936396.1	3.8	Methyl octadecyl ether	C19H40O	284.52	Lipophilic ether compound with reported antimicrobial properties	[22]
16.	17.7805	129003481.3	100.0	Diethyl Phthalate	C12H14O4	222.24	Plasticizer; reported antimicrobial and solvent properties	[22]
17.	18.5979	1602532.8	1.2	Cyclohexane, decyl-	C16H32	224.43	Hydrocarbon compound reported in fungal extracts	[22]
18.	18.9747	3574971.9	2.8	n-Hexyl salicylate	C13H18O3	222.28	Antimicrobial, fragrance, and antioxidant properties	[22]
19.	19.1074	1189208.3	0.9	3,4-Dihydroisoquinolin-7-ol, 6-	C9H11NO	149.19	Isoquinoline derivative with possible neuroprotective and antioxidant activity	[22]
20.	20.4396	3970396.2	3.1	Behenic alcohol	C22H46O	326.60	Emollient and anti-inflammatory activity	[22]
21.	20.5245	3866434.1	3.0	Pentacosane	C25H52	352.69	Antioxidant, antimicrobial, and insecticidal activity	[22]
22.	22.2123	14904332.3	11.6	Lidocaine	C14H22N2O	234.34	Local anesthetic; anti-inflammatory and analgesic activity	[22]
23.	22.4830	22271819.8	17.3	Pentadecanoic acid, 13-methyl-, methyl ester	C17H34O2	270.45	Fatty acid ester with antimicrobial and anti-inflammatory potential	[22]

24.	23.2632	3973250.6	3.1	1,2-Benzenedicarboxylic acid,	C8H6O4	166.13	Reported antimicrobial and plasticizer-related applications	[22]
25.	23.5657	3188490.2	2.5	Cyclodecasiloxane, eicosamethyl-	C20H60O10Si10	741.55	Silicone-based compound used in pharmaceutical formulations	[22]
26.	23.8099	9611571.8	7.5	Hexadecanoic acid, ethyl ester	C18H36O2	284.48	Antioxidant, anti-inflammatory, and antimicrobial activity	[22]
27.	27.0739	14100563.1	10.9	Methyl stearate	C19H38O2	298.50	Anti-inflammatory and hypocholesterolemic potential	[22]
28.	27.2809	10579570.1	8.2	Cyclodecasiloxane, eicosamethyl-	C20H60O10Si10	741.55	Silicone-based compound used in pharmaceutical formulations	[22]
29.	28.5971	6265257.9	4.9	Octadecanoic acid, ethyl ester	C20H40O2	312.53	Antioxidant and anti-inflammatory activity	[22]
30.	30.4016	13772034.4	10.7	Cyclononasiloxane, octadecamethyl-	C18H54O9Si9	667.43	Silicone compound with pharmaceutical formulation applications	[22]
31.	33.5808	14746143.7	11.4	Cyclodecasiloxane, eicosamethyl-	C20H60O10Si10	741.55	Silicone-based pharmaceutical excipient	[22]
32.	36.1655	9764004.8	7.6	N-(1-Methyl-2-[(trimethylsilyl)oxy]-2-{4-[(trimethylsilyl)oxy]phenyl} ethyl)- 4-phenylbutan-2-amine	C27H45NO2Si2	471.83	Silylated amine derivative; possible bioactive alkaloid-related activity	[22]
33.	37.3491	11710421.4	9.1	Cyclodecasiloxane, eicosamethyl-	C20H60O10Si10	741.55	Silicone-based compound used in pharmaceutical formulations	[22]
34.	38.9361	2904735.4	2.3	7,11-Dioxapentacyclo[15.3.0.0(4,16).0(5,13).0(	C20H28O4	332.43	Polycyclic oxygenated compound with possible	[22]

				5,10)]eicos-13-en-20-ol-8-one, 1.beta.,12,12-trimethyl-			antioxidant activity	
35.	39.6102	7617962.5	5.9	Cyclodecasiloxane, eicosamethyl-	C20H60O10Si10	741.55	Silicone-based compound with formulation applications	[22]
36.	41.2240	3984085.5	3.1	Cyclodecasiloxane, eicosamethyl-	C20H60O10Si10	741.55	Silicone-based compound with formulation applications	[22]

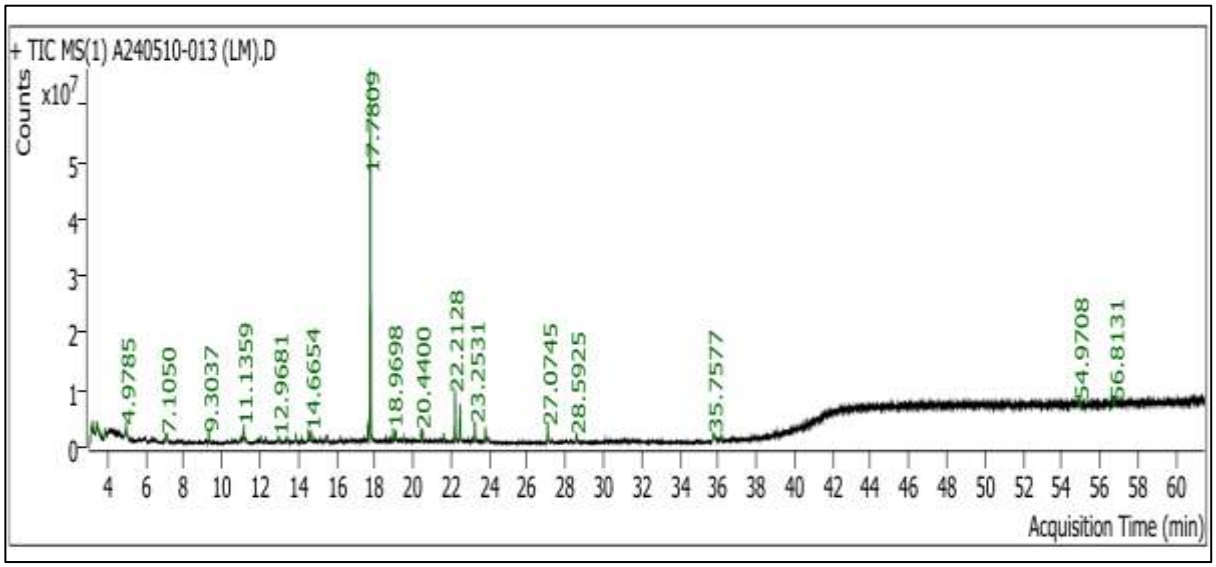

Figure-3 graphical representation of bioactive compounds identified by GC-MS in *Hieracium Erinaceus*

Table-2 GC–MS chromatogram of H. erinaceus mycelial extract showing the presence of key bioactive compounds.

Peak	Retention Time	Area	Area %	Compound Name	Molecular formula	Molecular weight	Compound activity	references
1.	3.1943	14239320.0	10.0	Benzene, 1,1'-[3-(3-cyclopentylpropyl)-1,5-pentanediyl]bis-	C25H34	334.54	Aromatic hydrocarbon with possible antimicrobial and hydrophobic interactions	[22]
2.	3.4406	14101676.9	9.9	Benzeneethanol, .alpha.-methyl-	C9H12O	136.19	Antimicrobial and aromatic alcohol activity	[22]
3.	3.8731	4731853.6	3.3	1,3-Cyclopentadiene, 5-(1-methylethylidene)-	C8H10	106.17	Unsaturated hydrocarbon reported in volatile bioactive fractions	[22]
4.	4.9785	9508494.3	6.7	Propane, 1-iodo-2-methyl-	C4H9I	184.02	Halogenated hydrocarbon; pharmaceutical intermediate	[22]

5.	7.1050	770470 2.5	5.4	Mesitylene	C9H12	120.19	Aromatic hydrocarbon with antioxidant-related applications	[22]
6.	9.3037	416905 5.8	2.9	Linalool	C10H18O	154.25	Anti-inflammatory, antioxidant, and antimicrobial activity	[22]
7.	11.1359	111396 29.1	7.8	Benzene, (iodomethyl)-	C7H7I	218.03	Halogenated aromatic intermediate used in chemical synthesis	[22]
8.	12.0309	260430 3.0	1.8	Benzaldehyde, 4-(1-methylethyl)-	C10H12O	148.20	Antimicrobial and fragrance-associated activity	[22]
9.	12.2772	228039 0.9	1.6	Methane, triiodo-	CHI3	393.73	Antimicrobial and antiseptic applications	[22]
10.	12.9681	439413 3.8	3.1	1-(p-Tolyl)-2-imidazolidinone	C10H12N 2O	176.22	Heterocyclic compound with reported antimicrobial and pharmacologica l activity	[22]
11.	13.3969	329351 4.3	2.3	2,3-Dichlorobenzyl alcohol, methyl ether	C8H8Cl2 O	191.05	Antimicrobial and aromatic ether-related activity	[22]
12.	13.8586	388705 1.9	2.7	Benzene, 1,2,3-trichloro-4- methyl-	C7H5Cl3	195.47	Halogenated aromatic compound; industrial intermediate	[22]
13.	14.5327	342440 1.5	2.4	1-Heneicosanol	C21H44O	312.58	Fatty alcohol with antimicrobial and emollient properties	[22]
14.	14.6654	468901 1.2	3.3	Decanamide, N-(2-hydroxyethyl)-	C12H25N O2	215.33	Surfactant-like molecule with antimicrobial potential	[22]
15.	15.4721	275325 4.0	1.9	Cyclohexane, octyl-	C14H28	196.37	Hydrocarbon compound identified in fungal extracts	[22]
16.	15.5146	219365 3.3	1.5	Quinoline, 1,2-dihydro-2,2,4-trimethyl-	C12H15N	173.25	Quinoline derivative with anti-inflammatory, antioxidant, and therapeutic potential	[22]
17.	17.6482	545477 9.4	3.8	Eicosyl acetate	C22H44O 2	340.58	Fatty acid ester with antimicrobial	[22]

							and emollient properties	
18.	17.7809	142164371.9	100.0	Diethyl Phthalate	C12H14O4	222.24	Plasticizer; reported antimicrobial and solvent-related activity	[22]
19.	18.9698	4565708.9	3.2	n-Hexyl salicylate	C13H18O3	222.28	Antioxidant, antimicrobial, and fragrance-related activity	[22]
20.	19.1078	3670014.2	2.6	1,2,3,4-Tetrahydroisoquinoline, 6,7,8-trimethoxy-1,2-dimethyl-	C14H21NO3	251.32	Isoquinoline derivative with neuroprotective and antioxidant potential	[22]
21.	19.5165	1237142.2	0.9	2,6-Di-tert-butyl-4-methoxyphenol, trifluoroacetate	C16H23F3O3	320.35	Potent antioxidant and free radical scavenging activity	[22]
22.	20.4400	4058685.5	2.9	Bacteriochlorophyll-c-stearyl	Approx. C55H74MgN4O6	Approx. 911.5	Photosynthetic pigment derivative with antioxidant potential	[22]
23.	20.5250	3027918.1	2.1	Pentacosane	C25H52	352.69	Antioxidant, antimicrobial, and insecticidal activity	[22]
24.	21.6077	3891447.0	2.7	Phthalic acid, butyl 3-(2-methoxyethyl)heptyl ester	C22H34O6	394.50	Plasticizer-like compound; hydrophobic bioactive properties	[22]
25.	22.2128	24249833.5	17.1	Lidocaine	C14H22N2O	234.34	Local anesthetic with anti-inflammatory and analgesic activity	[22]
26.	22.4782	19437565.0	13.7	Hexadecanoic acid, methyl ester	C17H34O2	270.45	Antioxidant, anti-inflammatory, antimicrobial activity	[22]
27.	23.2531	10593442.1	7.5	1,2-Benzenedicarboxylic acid, butyl 8-methylnonyl ester	C21H32O4	348.48	Ester compound with antimicrobial and hydrophobic properties	[22]
28.	23.8051	8248853.1	5.8	Hexadecanoic acid, ethyl ester	C18H36O2	284.48	Anti-inflammatory, antioxidant, antimicrobial activity	[22]
29.	27.0745	10721742.8	7.5	Methyl stearate	C19H38O2	298.50	Hypocholesterolemic and anti-inflammatory potential	[22]
30.	28.5925	4338582.6	3.1	Octadecanoic acid, ethyl ester	C20H40O2	312.53	Antioxidant and anti-	[22]

							inflammatory activity	
31.	35.7577	8945080.7	6.3	Hexadecanoic acid, 2-hydroxy-1-(hydroxymethyl)ethyl ester	C19H38O4	330.50	Emollient, antioxidant, and antimicrobial potential	[22]
32.	36.1558	3520010.1	2.5	Oxalic acid, mono-(5-[(2-bromophenyl)(2,2-dimethylpropionyloxy)methyl]-7,8-dihydro-5H-[1,3]dioxolo[4,5-g]isoquinolin-6-yl) ester	Approx. C24H24BrNO8	Approx. 534.35	Isoquinoline-associated heterocyclic compound with potential pharmacological activity	[22]
33.	54.9708	7379102.2	5.2	Octasiloxane,	C16H48O7Si8	578.99	Silicone-based compound commonly detected in GC–MS analysis	[22]

3.2 Target Prediction and Disease Gene Identification

Potential target genes associated with quinoline were retrieved from the Comparative Toxicogenomics Database (CTD). Target prediction analysis identified multiple protein targets associated with quinoline. Simultaneously, NAFLD-related genes retrieved from the CTD database highlighted several inflammatory and metabolic regulators involved in disease progression. Comparative analysis revealed overlapping targets potentially associated with the therapeutic activity of quinoline against NAFLD.

The identified targets were primarily associated with inflammatory signalling, oxidative stress response, lipid metabolism, and cytokine-mediated pathways, indicating the multi-target therapeutic potential of quinoline. Total 69 genes were chosen whose interaction was more than 1.

Table 3- showing all the identified genes from CTD database

s.no	Gene Symbol	Gene ID	Interaction
1.	TP53	7157	4
2.	CDKN2A	1029	3
3.	DNMT1	1786	3
4.	TIMP3	7078	3
5.	CDKN1A	1026	2
6.	CYP2E1	1571	2
7.	ESR1	2099	2
8.	LMNA	4000	2
9.	MAP3K20	51776	2
10.	MAP3K8	1326	2
11.	MAPK8	5599	2
12.	TNF	7124	2
13.	ACOT7	11332	1
14.	AIF1	199	1
15.	ANP32A	8125	1
16.	ANXA1	301	1
17.	ANXA2	302	1
18.	BTF3	689	1
19.	CASP3	836	1
20.	CBX3	11335	1
21.	CCNB1	891	1
22.	CNDP2	55748	1
23.	CSDE1	7812	1
24.	CYP1A2	1544	1
25.	CYP2A6	1548	1
26.	DNMT3A	1788	1
27.	DNMT3B	1789	1
28.	E2F1	1869	1
29.	EEF1G	1937	1

30.	EEF2	1938	1
31.	F2R	2149	1
32.	FSCN1	6624	1
33.	FUBP1	8880	1
34.	GRM1	2911	1
35.	HNRNPD	3184	1
36.	HNRNPL	3191	1
37.	ITGA5	3678	1
38.	ITGB3	3690	1
39.	LGALS3	3958	1
40.	LTA4H	4048	1
41.	MAP2K1	5604	1
42.	MET	4233	1
43.	MLH1	4292	1
44.	MTHFD2	10797	1
45.	NACA	4666	1
46.	NAMPT	10135	1
47.	NME2	4831	1
48.	OLA1	29789	1
49.	PAICS	10606	1
50.	PDAP1	11333	1
51.	PDHA1	5160	1
52.	PLPBP	11212	1
53.	PPARA	5465	1
54.	PPARG	5468	1
55.	PRKAR1A	5573	1
56.	PSMA3	5684	1
57.	PSMC1	5700	1
58.	PSMC5	5705	1
59.	PSMD4	5710	1
60.	PSMD7	5713	1
61.	RANBP1	5902	1
62.	RCN2	5955	1
63.	RRM1	6240	1
64.	SERPINB1	1992	1
65.	SERPINB5	5268	1
66.	TLR8	51311	1
67.	TXNDC5	81567	1
68.	WDR1	9948	1
69.	YBX1	4904	1

3.3 Protein–Protein Interaction Network Analysis

Protein–protein interaction (PPI) network analysis was performed to explore the relationships among the identified quinoline, target genes and to predict the biological pathways in which they may be involved. All selected targets were uploaded to the STRING database, with *Homo sapiens* specified as the reference organism, to construct the interaction network and evaluate their functional associations. The Protein–Protein Interaction network constructed using STRING database demonstrated strong interactions among the overlapping targets. Cytoscape analysis identified TNF-α as one of the major hub proteins exhibiting significant connectivity within the network. TNF-α plays a central role in mediating hepatic inflammation, insulin resistance, and progression of NAFLD toward steatohepatitis and fibrosis.

The identification of TNF-α as a hub target further supported its selection for molecular docking and simulation studies.

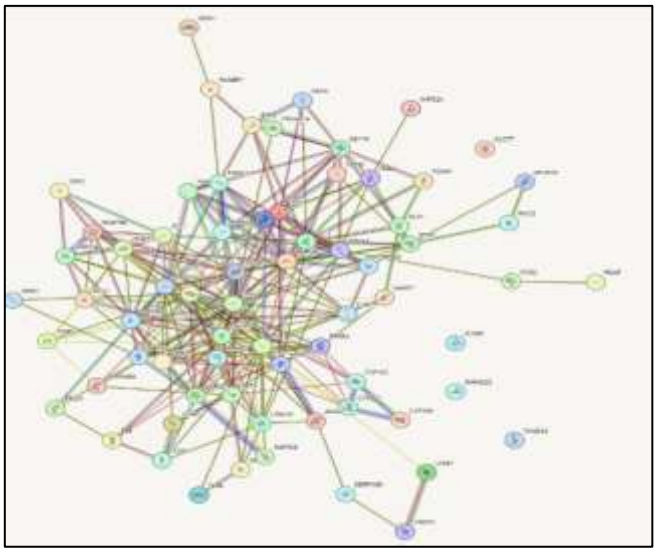

Figure 4- PPI network generated by STRING database illustrating number of nodes:69, number of edges: 288

3.4 Compound–Target–Pathway Interaction Network

The compound–target–pathway network was constructed and visualized using Cytoscape to investigate the interactions between quinoline, its associated target proteins, and enriched biological pathways. Network analysis revealed the multi-target pharmacological nature of quinoline, demonstrating its interactions with several proteins involved in inflammatory and metabolic regulation. Among the identified targets, TNF-α exhibited a prominent interaction profile, indicating its potential role as a key mediator of the therapeutic effects of quinoline. Furthermore, pathway analysis suggested that quinoline may influence inflammatory cytokine signaling and oxidative stress-related pathways, which are closely associated with hepatic injury and the progression of NAFLD.

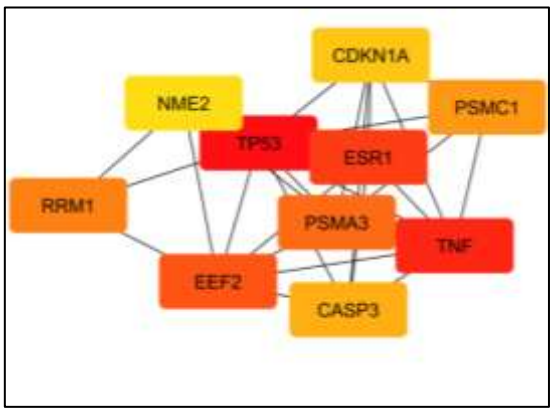

Figure 5- showing the visual representation of top ten targeted genes by using cytoscape tool

Table 4- Top 10 Ranked by Degree Method

Rank	Name	Score
1	TP53	38
2	TNF	33
3	ESR1	25
4	CASP3	24
5	CDKN1A	22
6	CDKN2A	18
7	EEF2	18
8	PPARG	16
9	HNRNPD	15
10	PSMA3	15

Table-5 Top 10 Ranked by Closeness Method

Rank	Name	Score
1	TP53	50.33333
2	TNF	47.66667
3	ESR1	43
4	CASP3	42.5

5	CDKN1A	41.16667
6	EEF2	40
7	HNRNPD	38.33333
8	CDKN2A	38.16667
9	PSMA3	38.16667
10	PPARG	37.5

Table-6 Top 10 Ranked by Betweenness Method

Rank	Name	Score
1	TP53	959.9526
2	TNF	875.7953
3	ESR1	356.0588
4	EEF2	355.4958
5	PSMA3	310.145
6	RRM1	305.3635
7	PSMC1	225.9042
8	CASP3	210.5442
9	CDKN1A	196.4459
10	NME2	142.2523

3.5 Functional Enrichment and Pathway Analysis

Gene Ontology enrichment analysis demonstrated that the identified targets were significantly enriched in biological processes related to inflammatory response, regulation of apoptosis, oxidative stress response, and lipid metabolic processes. Molecular function analysis indicated enrichment in cytokine receptor binding, enzyme regulation, and signalling receptor activity.

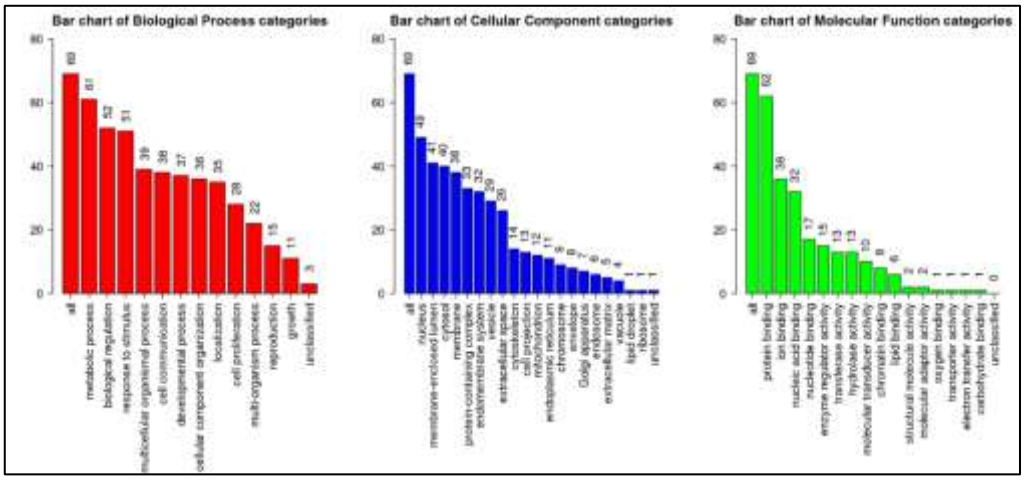

Figure 6- showing the graphical representation of biological process categories , cellular component categories , molecular function categories

KEGG pathway enrichment analysis revealed significant involvement of pathways associated with TNF signalling, NF-κB signalling, inflammatory response pathways, lipid metabolism, and oxidative stress regulation. These findings indicate that quinoline may exert therapeutic effects through modulation of multiple interconnected signalling pathways implicated in NAFLD pathogenesis.

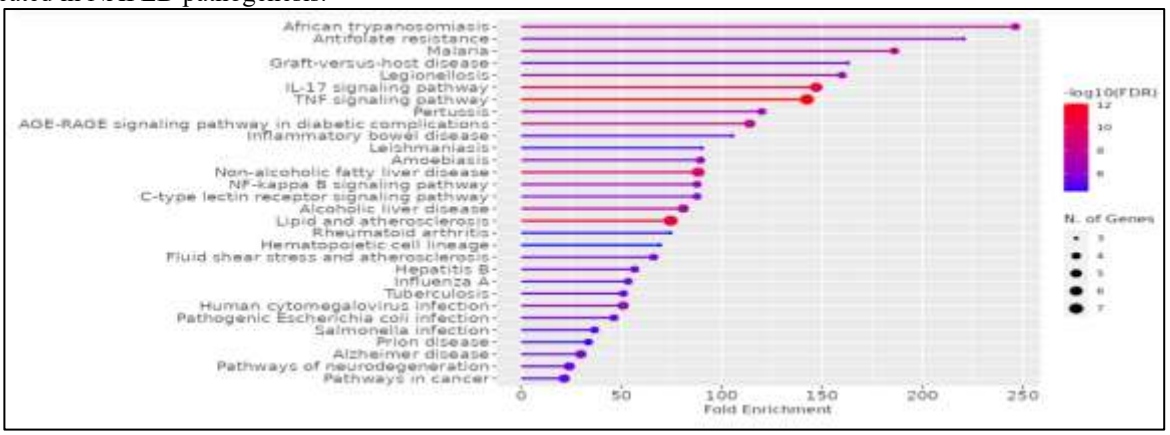

Figure 7- reprenstation of 69 tageted genes enriched with non- alcoholic liver disease and 29 other pathways

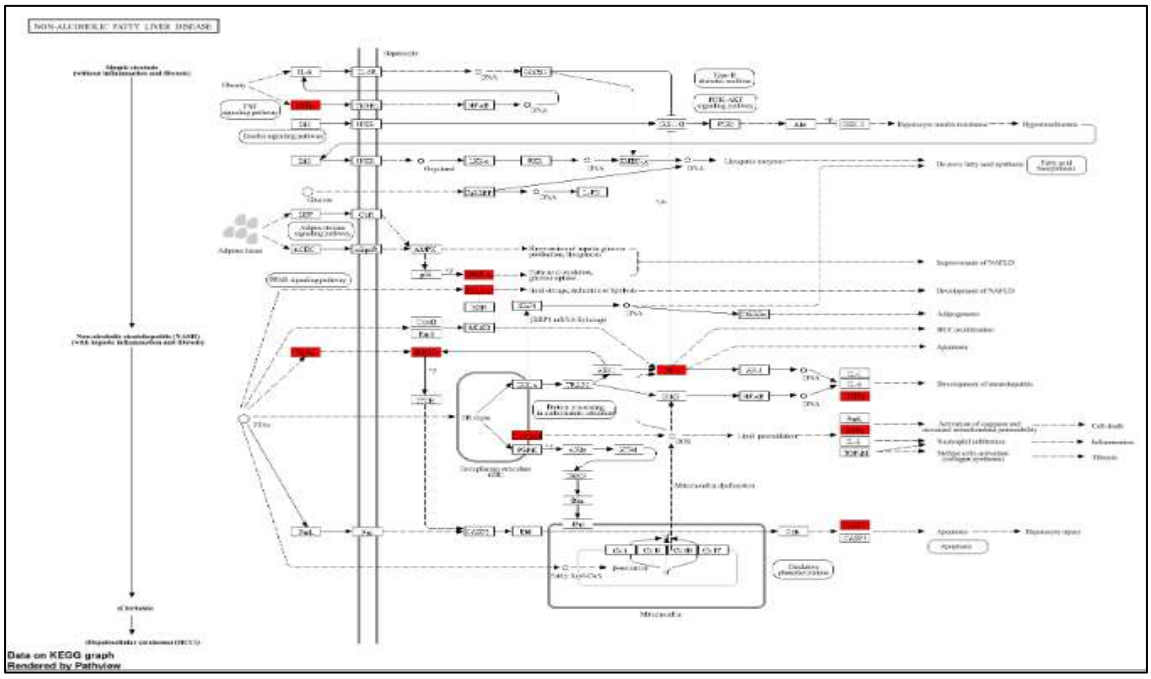

Figure 8 - showing that TNF is showing effectivity in treatment of Non-Alcoholic Liver Disease

3.6 Molecular Docking Analysis

Molecular docking analysis demonstrated favourable interaction between quinoline and TNF-α protein (PDB ID: 2AZ5). Quinoline exhibited a binding affinity score of −5.9 kcal/mol, indicating stable ligand–protein interaction.

The docked complex revealed that quinoline occupied the active binding pocket of TNF-α and established hydrophobic interactions with surrounding amino acid residues. The obtained binding affinity suggests that quinoline possesses potential inhibitory activity against inflammatory signalling mediated by TNF-α.

The docking of quinoline was performed with 2AZ5 which is the TNF-alpha coding protein. Ligand 2AZ5 with TNF-alpha gene coding protein , quinoline has the -5.9 6.0kcal/mol affinity which results that quinoline may have the potential of being a drug on non-alcoholic liver disease. The molecular docking analysis of the FDA-approved drugs **lenalidomide, omeprazole, and rabeprazole** was also performed for comparative evaluation. The docking results demonstrated that **quinoline** exhibited a stronger binding affinity toward the target protein than the selected FDA-approved drugs, suggesting its potential as a promising therapeutic candidate for the management of NAFLD.

Table 7- docking interaction of quinoline with other FDA approved drugs

Docking interaction		Affinity
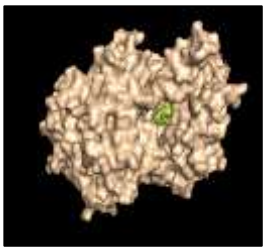 (A)QUINOLINE	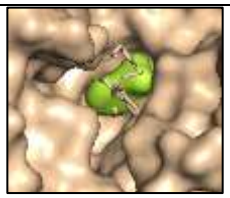	-5.9
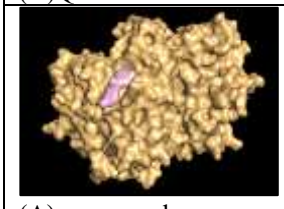 (A)omeprazole	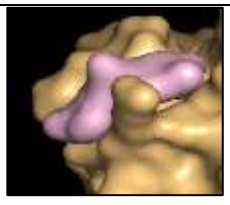	-5.6

 (B)Lenalidomide		-5.7
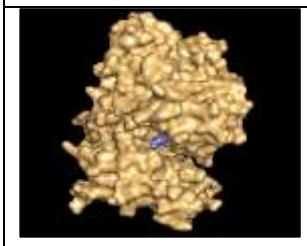 (D) rabeprazole	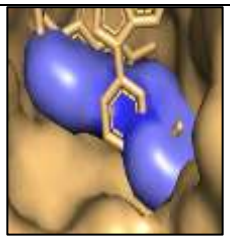	-5.9

Figure 9 (A) ligand protein interaction (2AZ5 (quinoline) in surface model, Figure9 (B) ligand protein interaction (2AZ5 (omeprazole) in surface model, Figure 9 (C) ligand protein interaction (2AZ5 (linalidomide) in surface model, 2AZ5ligand protein interaction 9 (D)(2Znn (rabeprazole) in surface model.

3.7 Molecular Dynamics Simulation Analysis

To validate the stability of the docked complex under dynamic physiological conditions, a 200 ns molecular dynamics simulation was performed.

3.7.1 RMSD Analysis

Root Mean Square Deviation (RMSD) analysis demonstrated that the TNF-α–quinoline complex remained structurally stable throughout the simulation period. Initial fluctuations were observed during equilibration; however, the system gradually achieved conformational stability, indicating stable protein–ligand interaction.

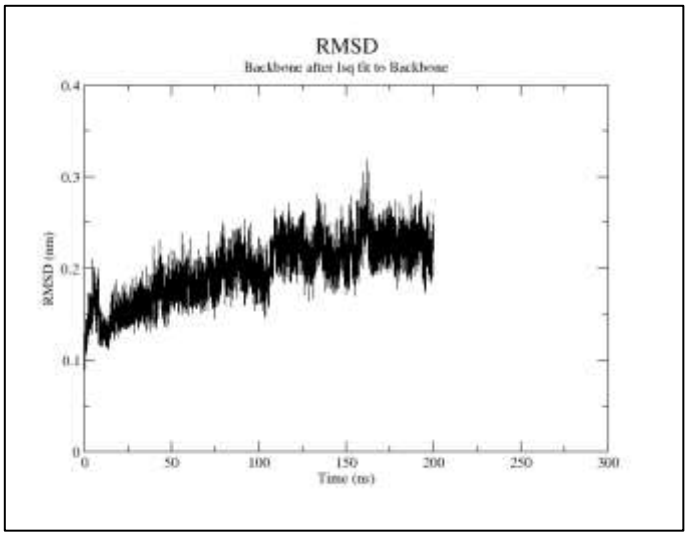

Figure 10: RMSD of protein in the complex (crystal, means original)

We can see that the RMSD of protein is fluctuating in accepted range (Figure 4). The calculated backbone RMSD value ranged from ~0.15 to ~0.3 nm approximately (accepted range) for the overall 200ns, suggesting that the protein structure is stable throughout 200ns. In conclusion, we can say that protein shows stability through the trajectory with insignificant conformational changes. This can be correlated with other parameters to confirm the stability like RMSF, Radius of gyration.

3.7.2 RMSF Analysis

Root Mean Square Fluctuation (RMSF) analysis revealed moderate flexibility in specific amino acid residues located primarily in loop regions, while the active site residues remained relatively stable. The observed fluctuations did not significantly affect the integrity of the binding complex. Root mean square fluctuations (RMSFs) measures the flexibility of each atom throughout the 200ns. Overall, the RMSF is showing low fluctuations that indicates that the protein backbone is stable with minimal conformational changes. While, few sharp peaks are observed around 290-300atoms, 1000-1300atoms, and 1400-1500atoms which shows flexible loop regions. Another peak is observed at 1200atoms (almost 1nm) which shows possible conformational rearrangement but since the remaining atom shows stability therefore, this

high pick is not significant enough for any unfolding in protein structure. Consistent with the RMSD analysis, RMSF results indicated the stable nature of complexes (Figure 11). The RMSF shows no significant impact on the peptide bonding

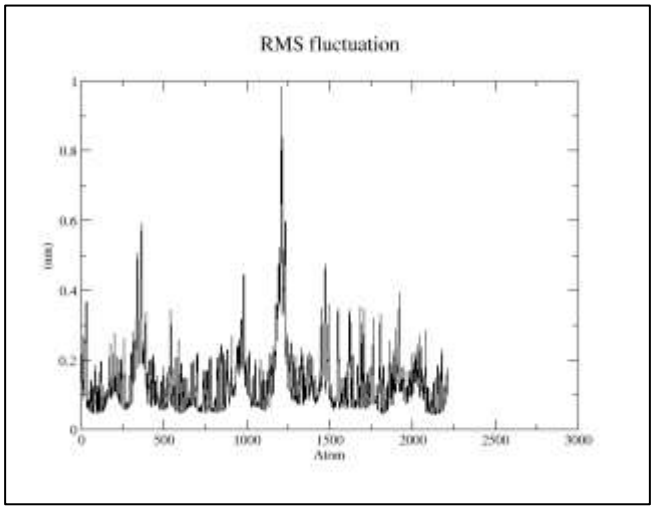

Figure 11: Root Mean Square Fluctuation

3.7.3 Radius of Gyration and SASA Analysis

Radius of gyration (Rg) analysis demonstrated maintenance of compact protein structure during the simulation. Solvent Accessible Surface Area (SASA) analysis indicated stable solvent exposure patterns without major conformational destabilization, suggesting preservation of structural integrity throughout the simulation.

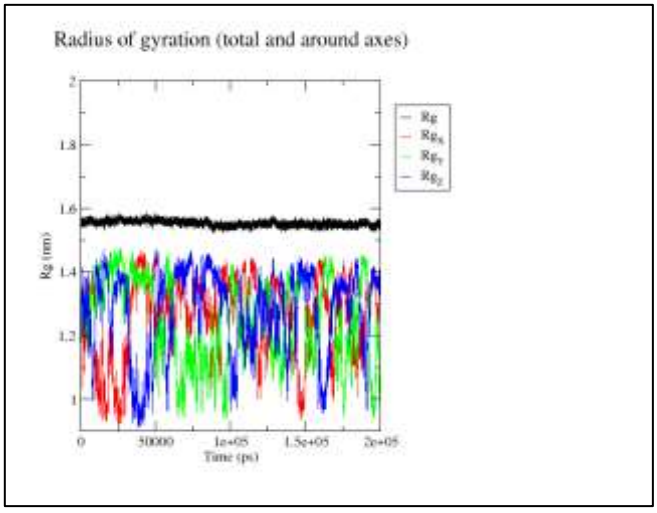

Figure 12: Radius of gyration

R_g is showing the regular stable graph hence the protein shows that it maintains its compactness.

SASA analysis assists in understanding the surface area of a protein that is accessible to solvent molecules, where more SASA shows, more surface is exposed to solvent or in other words, it shows how an amino acid interacts with its environment (solvent and protein) therefore both increase or decrease shows variations in the target amino acid residues. Figure 7 showed that SASA fluctuated approximately between 80-90nm^2 throughout the 200ns thus indicates conformational stability and stable dynamics of the protein.

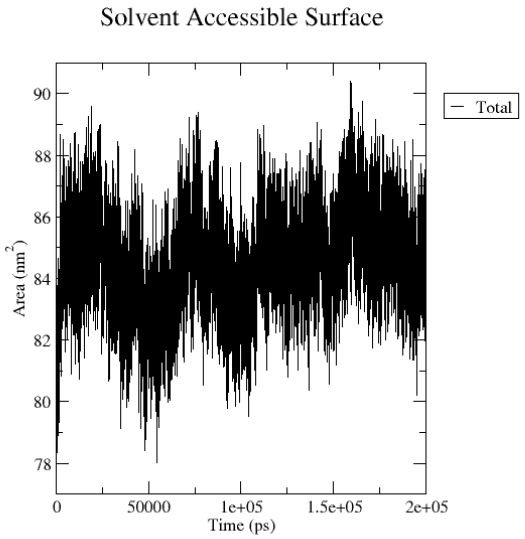

Figure 12: SASA analysis

3.7.4 Hydrogen Bond Analysis

Hydrogen bond analysis indicated minimal hydrogen bond formation between quinoline and TNF-α during the simulation trajectory. Nevertheless, hydrophobic and van der Waals interactions contributed significantly toward maintaining the stability of the complex.

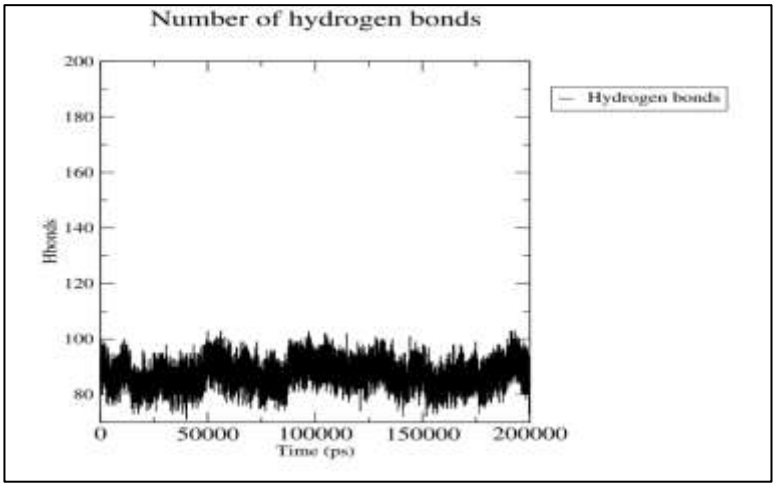

Figure 13: hydrogen bond formation in protein during simulation. We can observe ~75 and ~100 H-bonds throughout the simulation and there is no sharp drop or sudden increase, which indicates the protein structurally stable.

3.7.5 Principal Component Analysis and Free Energy Landscape

Principal Component Analysis (PCA) demonstrated restricted conformational motion of the protein–ligand complex, indicating dynamic stability during the simulation period. Free Energy Landscape (FEL) analysis further confirmed the presence of energetically favorable conformational states with stable minima, supporting the structural stability of the TNF-α–quinoline complex.

Overall, the MD simulation results demonstrated that quinoline maintained stable interaction with TNF-α throughout the 200 ns simulation period.

PCA analysis showed initial conformational adjustments followed by equilibration after ~60 ns, indicating attainment of a stable protein–ligand conformational state. Gradual transitions in PC1 and stabilized fluctuations in PC2 suggest adaptive but stable binding behaviour of quinoline within the protein binding pocket.

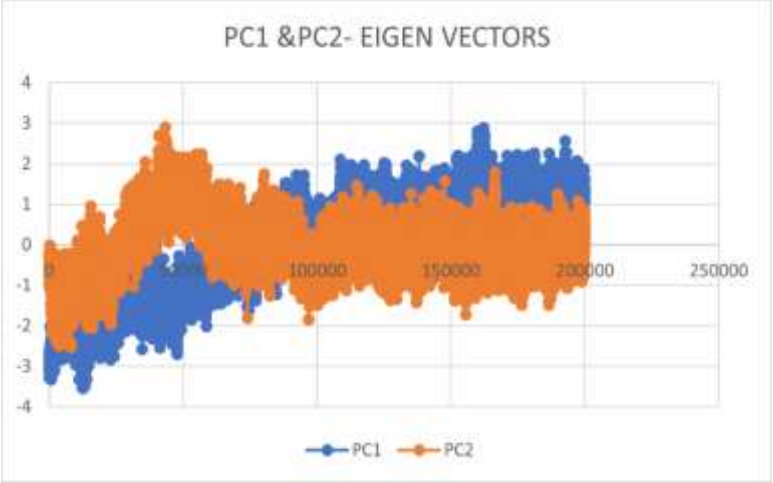

Figure 14: graphical representation of PCA1 and PCA 2

MMPBSA REPORT

Molecular Mechanics Poisson–Boltzmann Surface Area (MM/PBSA) calculations were performed using the gmx_MMPBSA tool to estimate the binding free energy (ΔG) of the protein–ligand complex. The individual energy components, including van der Waals, electrostatic, non-polar solvation, and total binding energy, are summarized in

Table 1: MM/PBSA Binding Free Energy Components of the Top Protein–Ligand Complex.

	Van der Waals energy (kcal/mol)	Electrostatic energy (kcal/mol)	Non-polar solvation energy (kcal/mol)	Free binding energy (kcal/mol)	Polar solvation energy (kcal/mol)
Complex	-13.59	-0.09	-1.86	-8.34	7.20
Percentage contribution %*	~162.95	~1.08	~22.30	100	~86.33
Role in binding	Dominant favorable contribution	Small contribution	Favorable contribution	Moderate to good	Unfavorable, opposes binding

*Percentage contribution= $\frac{\text{Energy Component}}{\text{Total energy}}$ *100

Binding Free Energy Deviation Analysis (ΔComplex)

This report summarizes the binding free energy decomposition results obtained from gmx_MMPBSA for the ΔComplex (Complex – Receptor – Ligand).

Table 2 – ΔComplex Energy Component Deviations

Energy Component	Average (kcal/mol)	SD(Prop.)	SD	SEM(Prop.)	SEM	Contribution
ΔVDWAALS	-13.59	0.28	1.81	0.03	0.18	Major favorable
ΔEEL	-0.09	0.85	0.4	0.09	0.04	Negligible/weak electrostatic interaction
ΔEGB	7.20	0.38	0.87	0.04	0.09	Major unfavorable
ΔESURF	-1.86	0.09	0.25	0.01	0.03	Moderate favorable
ΔTOTAL	-8.34	1.26	1.64	0.13	0.16	Moderate to good favorable
ΔBOND	-0.00	0.00	0.00	0.00	0.00	No contribution
ΔANGLE	0.00	2.69	0.00	0.27	0.00	No contribution
ΔDIHED	-0.00	1.15	0.00	0.12	0.00	No contribution
ΔGGAS	-13.68	1.20	1.80	0.12	0.18	Strong favorable
ΔGSOLV	5.34	0.39	0.72	0.04	0.07	Unfavorable

4. CONCLUSION

The present study employed an integrated computational approach to investigate the therapeutic potential of quinoline identified from the mycelial extracts of *Ganoderma lucidum* and *Hericium erinaceus* against Non-Alcoholic Fatty Liver Disease (NAFLD). Network pharmacology analysis revealed that quinoline may regulate multiple inflammatory and

metabolic pathways associated with NAFLD progression. Protein–protein interaction analysis identified TNF-α as a key hub target involved in hepatic inflammation and disease pathogenesis. Molecular docking analysis demonstrated favourable binding affinity between quinoline and TNF-α protein, while molecular dynamics simulation confirmed the structural stability of the complex over a 200 ns simulation period. Despite limited hydrogen bond interactions, the complex remained stable through hydrophobic and conformational interactions.The findings of this study suggest that quinoline possesses promising multi-target therapeutic potential against NAFLD and may contribute to the hepatoprotective properties of medicinal mushrooms. However, further in vitro and in vivo investigations are necessary to validate the pharmacological efficacy and molecular mechanisms of quinoline in experimental and clinical settings. The binding interaction is mainly driven by van der Waals interactions and gas phase energy, indicating dominant hydrophobic stabilization. Overall negative total binding energy suggests a thermodynamically favorable and stable complex (although we did not get any hydrogen bond in the complex) The major stabilizing contribution arises from the van der Waals interaction energy (**ΔVDWAALS = -13.59 kcal/mol**), suggesting that hydrophobic and dispersion interactions play a dominant role in complex stabilization. The electrostatic interaction energy (**ΔEEL = -0.09 kcal/mol**) contributes minimally to the overall binding affinity. The polar solvation energy (**ΔEGB = 7.20 kcal/mol**) opposes binding, which is commonly observed due to the energetic penalty associated with desolvation. The non-polar solvation energy (**ΔESURF = -1.86 kcal/mol**) contributes favorably toward stabilization of the complex. The gas-phase interaction energy (**ΔGGAS = -13.68 kcal/mol**) strongly favors binding, while the solvation contribution (**ΔGSOLV = 5.34 kcal/mol**) partially offsets this stabilization. The standard deviation (**SD = 1.64 kcal/mol**) indicates relatively stable energy fluctuations throughout the simulation trajectory. The standard error of the mean (**SEM = 0.16 kcal/mol**) demonstrates good statistical reliability and consistency of the calculated binding free energy values. Quinoline has an effect, non -alcoholic liver diseases, and its impact on non-alcoholic liver disease.These results shows that Quinoline can interact with various genes and proteins and pathways to form a systematic pharmacological network, Quinoline can be of good value if used in drug development and utilization. Limitations like skin sensitization, eye irritant respiratory toxicity, lesser oral bioavailability are barriers that has to be overcome in order to develop Quinoline as a dru

ACKNOWLEDGEMENT
The authors acknowledge the support provided by the Department of Biotechnology and associated laboratory facilities for conducting the present research work. The authors are also grateful to the Advanced Instrumentation Research Facility (AIRF), JNU, for GC-MS analysis support.

FUTURE PERSPECTIVES
Future studies should focus on experimental validation of quinoline through in vitro hepatocyte models and in vivo NAFLD animal studies to confirm its anti-inflammatory and hepatoprotective activities. Additionally, structural modification of quinoline derivatives may further enhance binding affinity and therapeutic efficacy against NAFLD-associated molecular targets.

REFERENCES
1. Paik, J.M., et al., *The burden of nonalcoholic fatty liver disease (NAFLD) is rapidly growing in every region of the world from 1990 to 2019.* Hepatology communications, 2023. **7**(10): p. e0251.
2. Motta, B.M., et al., *From non-alcoholic steatohepatitis (NASH) to hepatocellular carcinoma (HCC): epidemiology, incidence, predictions, risk factors, and prevention.* Cancers, 2023. **15**(22): p. 5458.
3. Nagata, N., et al., *An update on the chemokine system in the development of NAFLD.* Medicina, 2022. **58**(6): p. 761.
4. Manikanta, S.T., et al., *Mechanisms Of Organ Damage In Uncontrolled Diabetes: A Pathological Perspective.* cytokines, 2026. **1**: p. 3.
5. Karkucinska-Wieckowska, A., et al., *Mitochondria, oxidative stress and nonalcoholic fatty liver disease: A complex relationship.* European journal of clinical investigation, 2022. **52**(3): p. e13622.
6. Martín-Fernández, M., et al., *Role of oxidative stress and lipid peroxidation in the pathophysiology of NAFLD.* Antioxidants, 2022. **11**(11): p. 2217.
7. Vachliotis, I.D. and S.A. Polyzos, *The role of tumor necrosis factor-alpha in the pathogenesis and treatment of nonalcoholic fatty liver disease.* Current obesity reports, 2023. **12**(3): p. 191–206.
8. Bocca, C., et al., *Hepatic myofibroblasts: a heterogeneous and redox-modulated cell population in liver fibrogenesis.* Antioxidants, 2022. **11**(7): p. 1278.
9. Song, Z., et al., *The active components of traditional Chinese medicines regulate the multi-target signaling pathways of metabolic dysfunction-associated fatty liver disease.* Drug Design, Development and Therapy, 2025: p. 2693–2715.
10. Katiyar, D., et al., *Medicinal Mushrooms: Bioactive Components, Pharmacological, Immunological and Toxicological Insights.* ChemistrySelect, 2025. **10**(37): p. e01956.
11. 11. James, J., 2023. *Medicinal Mushrooms: The extraction and analysis of bioactive compounds from Hericium erinaceus and Ganoderma lucidum mushrooms* (Master's thesis, University of Windsor (Canada)).
12. Lull C, Wichers HJ, Savelkoul HF. Antiinflammatory and immunomodulating properties of fungal metabolites. Mediators of inflammation. 2005;2005(2):63-80.
13. Guo Y, Zhang M, Xu J, Dong M, Chen X, Yang A, Gao J, Yin X. Ganoapplanilactone C from Ganoderma applanatum Ameliorates Metabolic Dysfunction-Associated Steatotic Liver Disease via AMPK/mTOR-Mediated Lipid Regulation in Zebrafish. Antioxidants. 2025 May 26;14(6):637.

14. Bhardwaj N, Pathania A, Kumar P. Naturally available nitrogen-containing fused heterocyclics as prospective lead molecules in medicinal chemistry. Current Traditional Medicine. 2021 Feb 1;7(1):5-27.
15. Zhang SS, Tan QW, Guan LP. Antioxidant, anti-inflammatory, antibacterial, and analgesic activities and mechanisms of quinolines, indoles and related derivatives. Mini reviews in medicinal chemistry. 2021 Oct 1;21(16):2261-75.
16. Tanaka M, Szatmári I, Vécsei L. Quinoline quest: kynurenic acid strategies for next-generation therapeutics via rational drug design. Pharmaceuticals. 2025 Apr 22;18(5):607.
17. Singh N, Singh V, Prasad Singh M. In silico interactions of the biomolecules of edible mushrooms against lifestyle diseases. Mushrooms: a wealth of nutraceuticals and an agent of bioremediation. Bentham Science Publishers, Sharjah. 2023 Jun 12:80-95.
18. Zhu W, Li Y, Zhao J, Wang Y, Li Y, Wang Y. The mechanism of triptolide in the treatment of connective tissue disease-related interstitial lung disease based on network pharmacology and molecular docking. Annals of medicine. 2022 Dec 31;54(1):541-52.
19. Siddique S, Hussain K, Shehzadi N, Arshad M, Arshad MN, Iftikhar S, Saghir F, Shaukat A, Sarfraz M, Ahmed N. Design, synthesis, biological evaluation and molecular docking studies of quinoline-anthranilic acid hybrids as potent anti-inflammatory drugs. Organic & Biomolecular Chemistry. 2024;22(18):3708-24.
20. Rathi A, Wadhwa N, Jain CK, Bhatt E. Comparative Analysis of Bioactive Compounds of four edible Fungal Biomass by using GC-MS. InBIO Web of Conferences 2026 (Vol. 233, p. 02017). EDP Sciences.
21. Jopling DA. Paleo-medicine at Gesher Benot Ya'aqov. Evolution and Human Behavior. 2026 Mar 1;47(2):106807.
22. https://phytochem.nal.usda.gov/
23. Kim S, Chen J, Cheng T, Gindulyte A, He J, He S, Li Q, Shoemaker BA, Thiessen PA, Yu B, Zaslavsky L. PubChem 2025 update. Nucleic acids research. 2025 Jan 6;53(D1):D1516-25.
24. Bajpai, A.K., et al., *Systematic comparison of the protein-protein interaction databases from a user's perspective.* Journal of Biomedical Informatics, 2020. **103**: p. 103380.
25. Szklarczyk, D., et al., *The STRING database in 2017: quality-controlled protein–protein association networks, made broadly accessible.* Nucleic acids research, 2016: p. gkw937.
26. Li J, Su WW, Wang ZL, Ji XF, Wang JW, Wang K. Identification and verification of biomarkers associated with arachidonic acid metabolism in non-alcoholic fatty liver disease. Scientific Reports. 2025 Mar 12;15(1):8521.
27. Li Q, Sun H, Chen X, Chen C, Chen Y, He H, Yang F, Wang D, Zhou L. Integrative Network Pharmacology, Molecular Docking, and In Vitro Insights Into the Mechanism of Finger Citron for Non-Alcoholic Fatty Liver Disease. Food Science & Nutrition. 2026 Apr;14(4):e71695.
28. Zheng H, Li H, Du H, Sheng L, Huang N, Li X, Sun R. Unravelling the mechanisms of Erchen decoction in the treatment of nonalcoholic fatty liver disease (NAFLD): An integrative study combining network pharmacology, molecular docking, molecular dynamics simulation, multi-omics analysis, and experimental validation. Journal of ethnopharmacology. 2025 Sep 25;353:120216.
29. Yang R, Jiang D, Xu H, Yang H, Feng L, Wu Q, Xing Y. Network Pharmacology and molecular Docking integrated with molecular dynamics simulations investigate the Pharmacological mechanism of Yinchenhao Decoction in the treatment of Non-alcoholic fatty liver disease. Current Computer-Aided Drug Design. 2025 Aug;21(5):721-37.